



DEEP *CHANDRA* OBSERVATIONS OF THE COMPACT STARBURST GALAXY HENIZE 2–10: X-RAYS FROM THE MASSIVE BLACK HOLE

AMY E. REINES^{1,2,7}, MARK T. REYNOLDS², JON M. MILLER², GREGORY R. SIVAKOFF³, JENNY E. GREENE⁴,
RYAN C. HICKOX⁵, AND KELSEY E. JOHNSON⁶

¹National Optical Astronomy Observatory, 950 North Cherry Avenue, Tucson, AZ 85719, USA; reines@noao.edu

²Department of Astronomy, University of Michigan, 1085 South University Avenue, Ann Arbor, MI 48109, USA

³Department of Physics, University of Alberta, CCIS 4-181, Edmonton AB T6G 2E1, Canada

⁴Department of Astrophysical Sciences, Princeton University, Princeton, NJ 08544, USA

⁵Department of Physics and Astronomy, Dartmouth College, 6127 Wilder Laboratory, Hanover, NH 03755, USA

⁶Department of Astronomy, University of Virginia, P.O. Box 400325, Charlottesville, VA 22904-4325, USA

Received 2016 September 9; revised 2016 October 3; accepted 2016 October 4; published 2016 October 20

ABSTRACT

We present follow-up X-ray observations of the candidate massive black hole (BH) in the nucleus of the low-mass, compact starburst galaxy Henize 2–10. Using new high-resolution observations from the *Chandra X-ray Observatory* totaling 200 ks in duration, as well as archival *Chandra* observations from 2001, we demonstrate the presence of a previously unidentified X-ray point source that is spatially coincident with the known nuclear radio source in Henize 2–10 (i.e., the massive BH). We show that the hard X-ray emission previously identified in the 2001 observation is dominated by a source that is distinct from the nucleus, with the properties expected for a high-mass X-ray binary. The X-ray luminosity of the nuclear source suggests the massive BH is radiating significantly below its Eddington limit ($\sim 10^{-6} L_{\text{Edd}}$), and the soft spectrum resembles other weakly accreting massive BHs including Sagittarius A*. Analysis of the X-ray light curve of the nucleus reveals the tentative detection of a ~ 9 hr periodicity, although additional observations are required to confirm this result. Our study highlights the need for sensitive high-resolution X-ray observations to probe low-level accretion, which is the dominant mode of BH activity throughout the universe.

Key words: accretion, accretion disks – galaxies: active – galaxies: dwarf – galaxies: nuclei – X-rays: general

1. INTRODUCTION

Henize 2–10 is a remarkable compact starburst galaxy, hosting an abundance of young “super star clusters” (e.g., Johnson et al. 2000) and a candidate low-luminosity active galactic nucleus (AGN; Reines et al. 2011). The discovery of an AGN in Henize 2–10 provides an excellent opportunity to study black hole (BH) accretion and star formation in a nearby (~ 9 Mpc), low-mass ($\lesssim 10^{10} M_{\odot}$; Nguyen et al. 2014), gas-rich galaxy, as well as the potential formation of a nuclear star cluster around a preexisting massive BH (Nguyen et al. 2014; Arca-Sedda et al. 2015). Moreover, this finding has helped spark a number of recent searches for AGNs in dwarf galaxies (e.g., Reines et al. 2013, 2014; Baldassare et al. 2015, 2016; Lemons et al. 2015; Hainline et al. 2016), ultimately leading to the realization that massive BHs in dwarfs are much more common than previously thought (for a review, see Reines & Comastri 2016).

The evidence for a massive BH in Henize 2–10 comes from a wealth of multi-wavelength data (Reines et al. 2011), including Very Large Array (VLA) radio observations that reveal an unresolved non-thermal nuclear point source (also see Kobulnicky & Johnson 1999 and Johnson & Kobulnicky 2003). Very long baseline interferometry (VLBI) observations constrain the size of the nuclear radio emission to $< 1 \text{ pc} \times 3 \text{ pc}$ and the high brightness temperature of the radio core confirms a non-thermal origin (Reines & Deller 2012).

Chandra X-ray Observatory observations of Henize 2–10 taken in 2001 show point-like hard X-ray emission that has previously been associated with the nuclear radio source (Ott

et al. 2005; Kobulnicky & Martin 2010; Reines et al. 2011). Here, we demonstrate that this emission is dominated by a source that is highly variable (also see Whalen et al. 2015) and *not* in fact co-spatial with the radio source. Our new deep *Chandra* observations expose a different, previously unidentified X-ray counterpart to the nuclear radio source (Figure 1), for which we examine the X-ray spectrum and light curve.

2. OBSERVATIONS AND DATA REDUCTION

We obtained new *Chandra* observations of Henize 2–10 in 2015 February. The total exposure time of ~ 200 ks was broken up into two observations of 159,066 s and 37,577 s beginning on February 5 and 16 (PI: Reines, ObsIDs 16068 and 16069). These observations were taken in VFAINT mode. We also retrieved the archival observation taken on 2001 March 23 (PI: Martin, ObsID 2075), which was taken in FAINT mode with an exposure time of 19,755 s. In all three observations, the galaxy was placed on the S3 chip of the Advanced CCD Imaging Spectrometer (ACIS) detector. The data were reduced and reprocessed with CIAO version 4.6 (Fruscione et al. 2006) utilizing CALDB version 4.6.3. To improve the image quality, the data were reprocessed with the EDSEER algorithm enabled (Li et al. 2004) and subsequently rebinned to 1/8th the native ACIS pixel size before convolving with an FWHM = $0''.25$ Gaussian. Our spectral and variability analysis is performed on the event files.

To improve the astrometry, we co-aligned the three *Chandra* observations and then tied the corrected images to the absolute reference frame defined by our radio observations, which is accurate to $\lesssim 0''.1$ (Reines et al. 2011; Reines & Deller 2012). We first averaged the coordinates of a bright point source

⁷ Hubble Fellow.

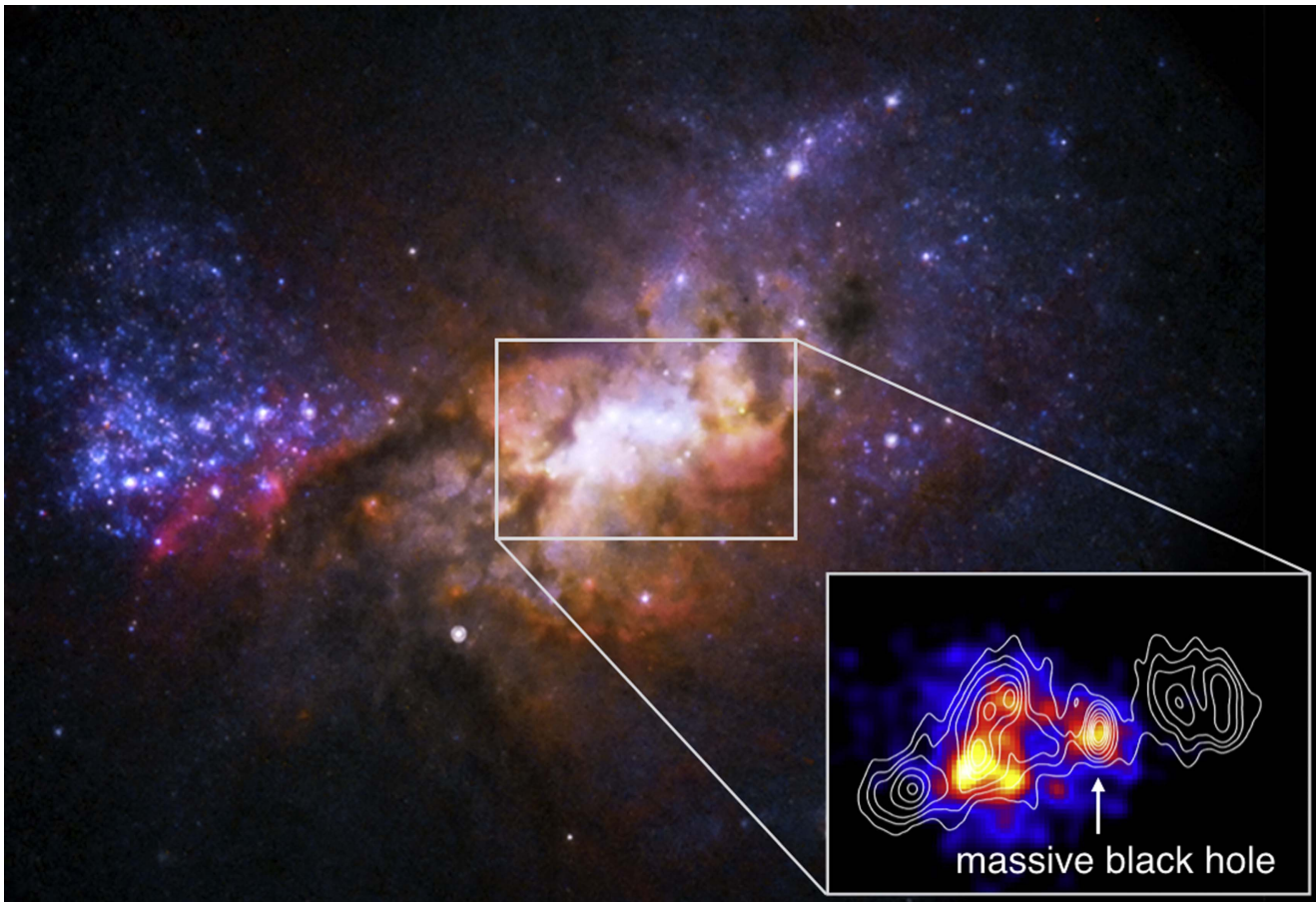


Figure 1. *HST* image of Henize 2–10. The inset shows our new 160 ks *Chandra* observation with VLA radio contours from Reines et al. (2011) and has dimensions $6'' \times 4''$ (~ 265 pc \times 175 pc).

common to all three *Chandra* observations, yet outside the vicinity of the nuclear region. This reference source is located $\sim 9''.5$ east of the nuclear radio source and has a corrected (mean) position of R.A. = 8:36:15.83, decl. = $-26:24:34.1$ (Figure 2). We then registered the three *Chandra* observations by determining the relative offset between this mean position and the position of the reference source in an individual observation. The required (R.A., decl.) shifts in arcseconds are ($0''.17$ W, $0''.13$ N), ($0''.08$ E, $0''.00$ S), and ($0''.08$ E, $0''.13$ S) for the 20 ks, 160 ks, and 40 ks observations, respectively. There is no evidence for significant rotation between the different observations. A comparison between our deep 160 ks observation and the VLA contours from Reines et al. (2011) indicates a close match between bright regions of X-ray and radio emission from recent star formation (inset Figure 1), strongly suggesting the absolute astrometry of our corrected *Chandra* observations is accurate and requires no additional shift. The absolute astrometric uncertainties of the final *Chandra* positions are estimated to be $0''.15$ in R.A. and $0''.13$ in decl. using the standard deviation of the three individual uncorrected measurements of the reference source.

3. ANALYSIS AND RESULTS

3.1. The Newly Identified Nuclear X-Ray Source

Our primary goal in this Letter is to examine the nuclear X-ray source in Henize 2–10. From Figures 1 and 2, we can now see that a previously unidentified X-ray source is spatially

coincident with the central radio source, hereafter referred to as the nuclear X-ray source (visible in the 160 ks image at R.A. = 8:36:15.12, decl. = $-26:24:34.1$), and that the bright X-ray emission identified in the 2001 observation (Ott et al. 2005; Kobulnicky & Martin 2010; Reines et al. 2011; Whalen et al. 2015) is dominated by an X-ray source (R.A. = 8:36:15.10, decl. = $-26:24:33.5$) distinct from the nuclear radio source. The spatial offset between the bright off-nuclear X-ray source in the subpixel image from 2001 and the VLBI position is $\sim 0''.7$ (~ 30 pc projected). This offset is significantly larger than our astrometric uncertainties, and thus our conclusion that the hard X-ray source is distinct from the nuclear radio source is secure. This source is also highly variable—it dominates the emission in 2001, is essentially absent in our new 160 ks observation, and returns in the 40 ks observation taken only 9 days later.

The spectrum of the bright, off-nuclear variable source dominating the 2001 observation is poorly constrained, but consistent with a highly absorbed power law ($N_H \sim 7 \times 10^{22}$ cm $^{-2}$, $\Gamma = 1.8$). Assuming a common spectral shape in each of the three observations, we measure unabsorbed 0.3–10.0 keV fluxes of $(5.09^{+1.68}_{-1.24}, 0.17^{+0.09}_{-0.07}, \text{ and } 1.28^{+0.47}_{-0.38}) \times 10^{-13}$ erg s $^{-1}$ cm $^{-2}$ respectively (90% confidence intervals), i.e., variability of a factor of ~ 30 . The large-amplitude variability (also see Whalen et al. 2015) and the large luminosity in the 2001 observation ($\geq 10^{39}$ erg s $^{-1}$) suggests it is an X-ray binary (XRB) containing a stellar-mass BH primary.

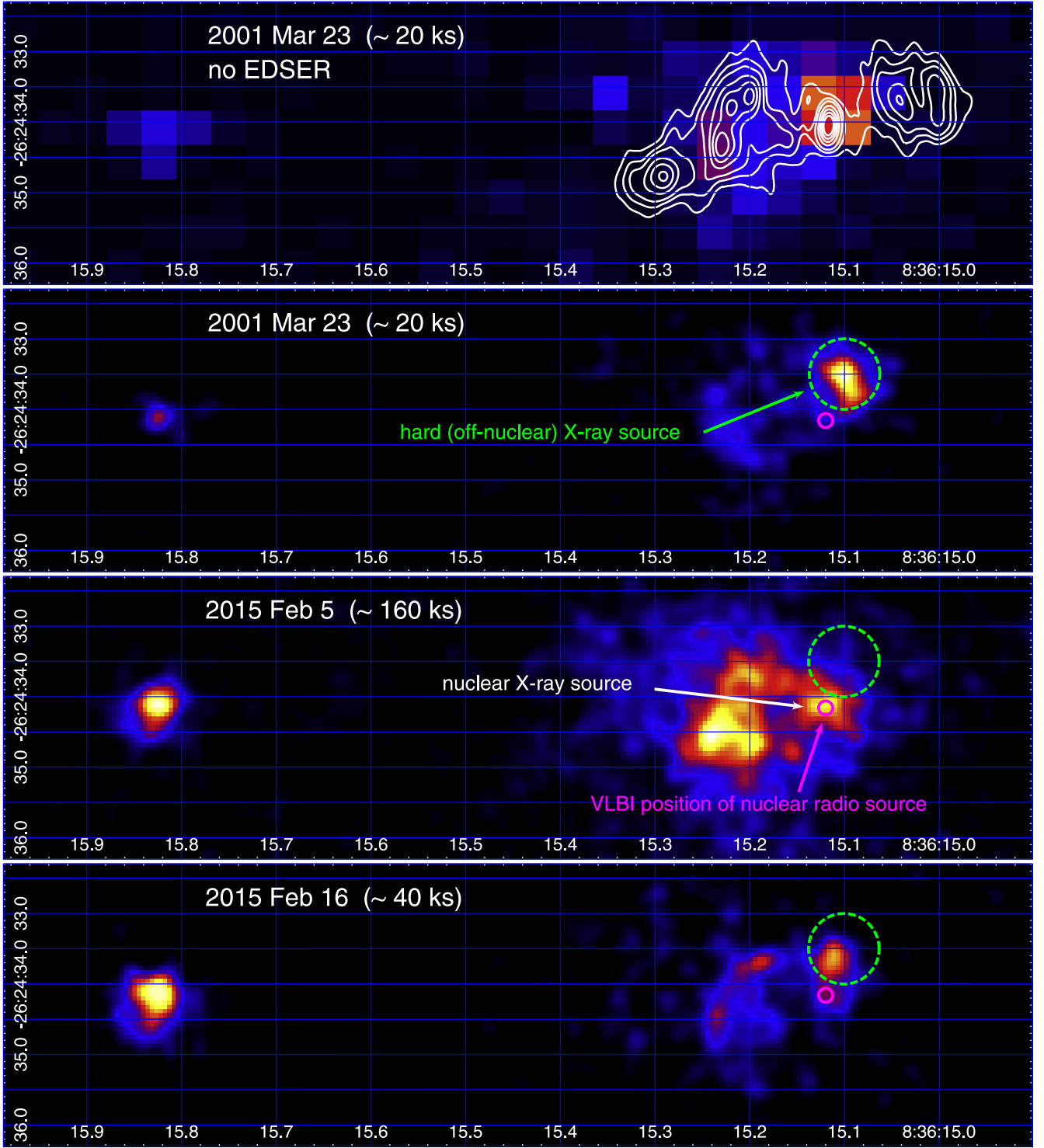


Figure 2. *Chandra* observations showing the central region of Henize 2–10. All images are in the 0.3–7 keV energy range but not on the same count rate scale. The top panel shows the observation from 2001 used by Reines et al. (2011) without the EDSEr algorithm enabled. VLA contours from Reines et al. (2011) are overlaid to show the seeming match between the bright hard X-ray source and the nuclear radio source. The bottom three panels show all observations using the EDSEr algorithm. The VLBI position and absolute positional uncertainty of the nuclear radio source from Reines & Deller (2012) are indicated by a magenta circle with $r = 0''.1$. The bright hard X-ray source previously identified in the 2001 observation (also seen in the 40 ks observation from 2015) is indicated by a green circle ($r = 0''.5$) and is clearly offset from the nuclear radio source. A newly revealed X-ray source visible in the 160 ks observation from 2015 is co-spatial with the nuclear radio source.

3.2. X-Ray Spectrum of the Nucleus

The fortuitous disappearance of the highly variable off-nuclear X-ray source in our 160 ks observation enables us to extract a relatively clean X-ray spectrum of the nuclear source. We extracted the spectrum in the 0.3–7.0 keV range from a circular

aperture with a radius of $0''.5$, correcting for the small aperture. The background was estimated from a source-free annular region extending from $20''$ to $25''$ centered on the nuclear source. We note that the external background contribution is negligible at the position of the nucleus; however, we cannot reliably separate

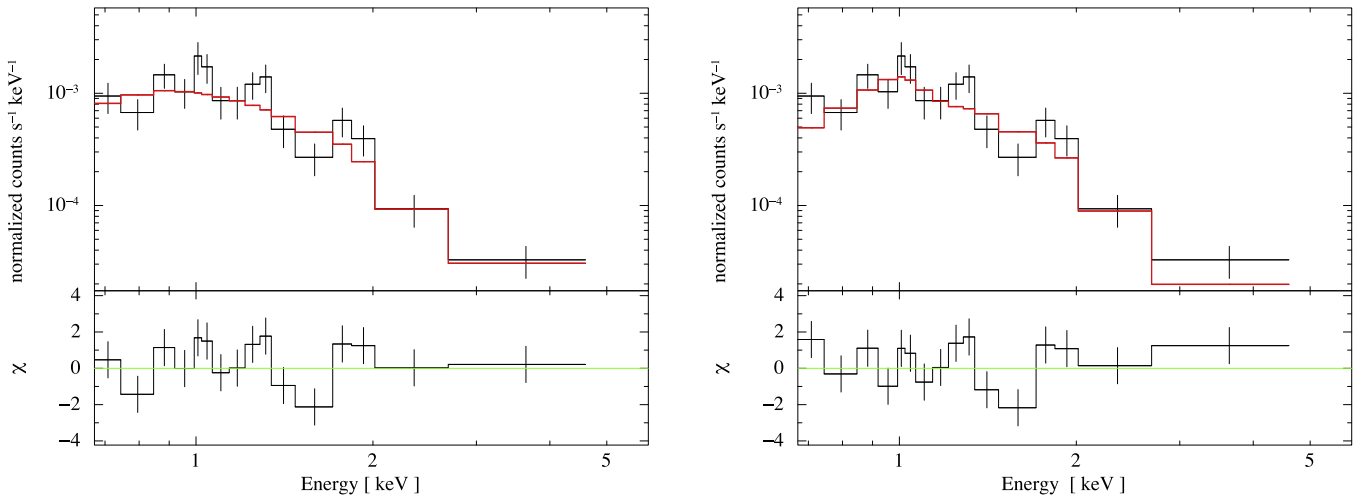


Figure 3. X-ray spectrum of the nuclear source. Best-fit power-law model (left) and best-fit thermal plasma model (right), with residuals shown beneath.

the point source from any local background within the source extraction region. We obtained a total of 183 net counts. The spectrum was grouped to have signal-to-noise ratio (S/N) = 3 per bin, and spectral fits to the background-subtracted spectrum were carried out within XSPEC 12.8.2q (Arnaud 1996) using the chi statistic and standard Gaussian weighting. Galactic foreground absorption was held fixed at $N_{\text{H,Gal}} = 9.1 \times 10^{20} \text{ cm}^{-2}$ (Kalberla et al. 2005) and the internal absorption was found to be negligible. We used the `phabs` absorption model, with abundances and cross-sections adopted from Asplund et al. (2009) and Balucinska-Church & McCammon (1992), respectively.

The source spectrum is well characterized by either an absorbed power-law model with photon index $\Gamma \sim 2.9$, or a thermal plasma model with $kT \sim 1.1 \text{ keV}$ (Figure 3, Table 1). Both models give a consistent intrinsic luminosity of $L_{0.3-10 \text{ keV}} \sim 10^{38} \text{ erg s}^{-1}$.

3.3. X-Ray Light Curve of the Nucleus

We also examine the temporal behavior of the nuclear X-ray emission during the 160 ks observation. Utilizing the same extraction regions as used for the spectral analysis, a background-subtracted light curve was created using DMEXTRACT. As the count rate is low, the light curve was extracted at 5 ks resolution and Gehrels errors are assumed (Gehrels 1986).

From Figure 4, we can see that the light curve exhibits clear variability (a factor of $\sim 2\times$) and the X-ray emission appears to oscillate within the 160 ks exposure. A model consisting of a constant plus a sine wave provides an excellent characterization of the light curve ($\chi^2/\nu = 9.2/29$) and reveals a best-fit period of $P = 33.5 \pm 2.6 \text{ ks}$ (90% confidence level). In the right panel of Figure 4, we plot the resulting light curve when folded on the detected period of $P = 33.5 \text{ ks}$ (9.3 hr). The amplitude of the sine model is $(4.71 \pm 1.22) \times 10^{-4} \text{ counts s}^{-1}$, and thus is measured to 3.9σ .

If instead the light curve is modeled as a constant, we obtain a best fit of $\chi^2/\nu = 18.4/32$. An F-test was used to determine that the sine model is a superior description of the data at the 99.9866% confidence level (3.8σ). This simple statistical test is dependent on the binning of the light curve, e.g., a binning of 3/10 ks resolution favors a sine wave over a constant model at the 95.7%/99.3% level with $P = 33.4 \pm 2.2 \text{ ks}$, $33.8 \pm 1.9 \text{ ks}$,

Table 1
Spectral Fits to the Nuclear X-Ray Source in Henize 2–10

Power-law Model	
χ^2/dof	22.40/14
Γ	$2.93^{+0.36}_{-0.33}$
Normalization ($10^{-6} \text{ photons cm}^{-2} \text{ s}^{-1} \text{ keV}^{-1}$ at 1 keV)	4.30 ± 0.66
$F_{0.3-10 \text{ keV}}$ ($10^{-14} \text{ erg s}^{-1} \text{ cm}^{-2}$), absorbed	$1.30^{+0.22}_{-0.17}$
$\log L_{0.3-10 \text{ keV}}$ (erg s^{-1}), unabsorbed	$38.10^{+0.07}_{-0.06}$
Thermal Plasma Model (APEC)	
χ^2/dof	22.64/13
kT (keV)	$1.06^{+0.27}_{-0.19}$
$Z (Z_{\odot})$	$0.06^{+0.16}_{-0.06}$
Normalization ($\frac{10^{-14}}{4\pi [D_A(1+z)]^2 \int n_e n_H dV}$)	$1.97^{+0.87}_{-0.73}$
$F_{0.3-10 \text{ keV}}$ ($10^{-14} \text{ erg s}^{-1} \text{ cm}^{-2}$), absorbed	$0.89^{+0.12}_{-0.28}$
$\log L_{0.3-10 \text{ keV}}$ (erg s^{-1}), unabsorbed	$37.94^{+0.05}_{-0.16}$

Note. We adopt $N_{\text{H,Gal}} = 9.1 \times 10^{20} \text{ cm}^{-2}$ due to the Milky Way and $N_{\text{H}} = 1 \times 10^{20} \text{ cm}^{-2}$ intrinsic to Henize 2–10. The errors represent the 90% confidence interval for one interesting parameter determined using the `error` command in XSPEC.

respectively. However, the best-fit period is robustly determined irrespective of the actual binning.

The power spectrum also hints at the presence of a periodic signal. Utilizing the entire observation at the native temporal resolution ($\Delta t = 3.14104 \text{ s}$) reveals the presence of a low significance peak ($\lesssim 2\sigma$) at a frequency $f \sim 3 \times 10^{-5} \text{ Hz}$ ($P \sim 33 \text{ ks}$) on top of a white noise background. If the signal is in fact periodic, the detected peak in the power spectrum is likely of low statistical significance due to the small number of cycles sampled in our 160 ks observation ($\lesssim 5$). However, we cannot rule out the possibility that the seemingly periodic signal could be produced by stochastic variability, which can sometimes mimic intervals of periodicity (e.g., “red noise”; Vaughan & Uttley 2006; Vaughan et al. 2016).

The oscillating signal is uniquely coincident with the nuclear source as identified in our subpixel spatial analysis. We have examined light curves from the bright region $2''$ to the east and find no evidence for any significant periodic signal at this location only 3 ACIS-S pixels from the nucleus. Likewise,

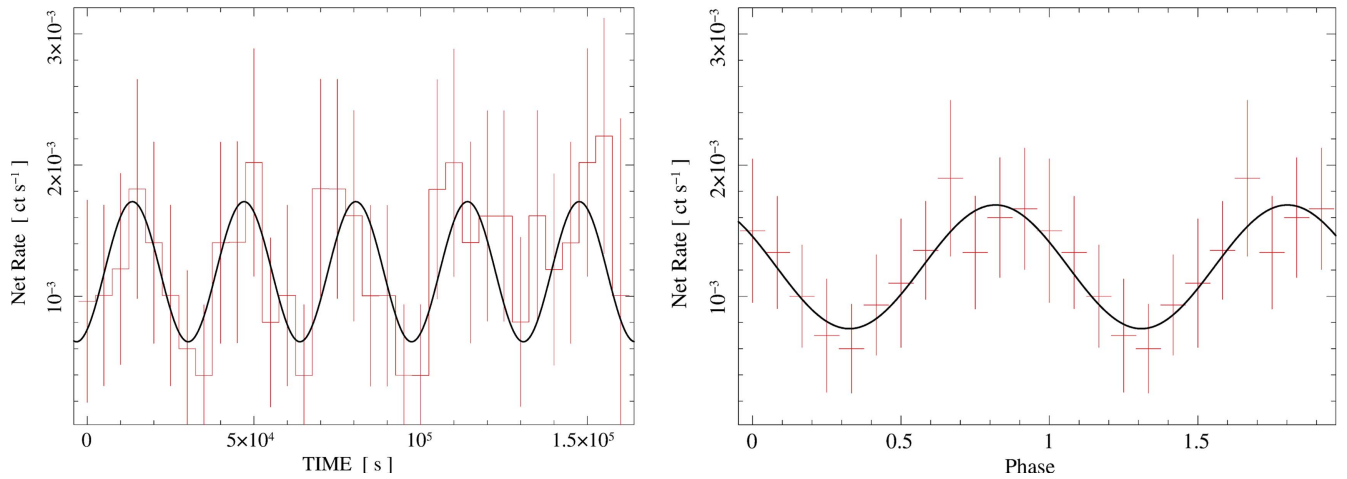


Figure 4. Oscillating X-ray emission from the nuclear source. Left: light curve binned at 5 ks resolution with the best-fit sine model overplotted. Right: light curve folded on the best-fit period of $P = 33.5$ ks and rebinned to 12 bins per cycle. Two cycles are displayed for clarity.

analysis of the light curves of the remaining point sources on the ACIS-S3 detector reveals no evidence for periodicity. Neither do we observe significant background flaring or the presence of periodic variability in the background signal on the ACIS-S3 detector during this observation. A period of ~ 33 ks should also not be due to aspect dithering.

4. DISCUSSION

We have shown that a previously unidentified *Chandra* X-ray point source is spatially coincident ($\lesssim 0''.1$, $\lesssim 5$ pc projected) with the non-thermal compact nuclear radio source in Henize 2–10 (Reines & Deller 2012). Using three separate *Chandra* observations and improved image processing, we have determined that the bright hard X-ray source that dominated the original 2001 observation (Ott et al. 2005; Kobulnicky & Martin 2010; Reines et al. 2011; Whalen et al. 2015) is distinct and spatially offset from the nuclear radio source. The previously detected hard X-ray source is highly variable with properties expected for a stellar-mass BH XRB. Fortunately, this source was absent in our new 160 ks observation, which enabled us to extract and analyze a clean spectrum and light curve of the newly revealed nuclear X-ray source.

Our new results from *Chandra* support a massive BH origin for the nuclear source in Henize 2–10 (Reines et al. 2011). Given a recent estimate for the total stellar mass of Henize 2–10 ($M_* \sim 10^{10} M_\odot$; Nguyen et al. 2014), we expect a nuclear BH with a mass⁸ of $M_{\text{BH}} \sim 3 \times 10^6 M_\odot$ (Reines & Volonteri 2015), although the uncertainty is at least a factor of a few. The luminosity of the nuclear X-ray source is $L_{0.3-10 \text{ keV}} \sim 10^{38} \text{ erg s}^{-1}$. This implies an Eddington ratio of $\sim 10^{-6}$, assuming an X-ray to bolometric correction of ~ 10 (e.g., Vasudevan & Fabian 2009). The X-ray spectrum is soft and can be well fit by either a thermal plasma model with $kT \sim 1.1$ keV or a power-law model with $\Gamma \sim 2.9$, similar to Sagittarius A* at the center

of the Milky Way (Baganoff et al. 2003) and other massive BHs accreting at very low Eddington ratios (e.g., Constantin et al. 2009). The presence of a spatially coincident non-thermal radio source, with a physical size of $\lesssim 1 \text{ pc} \times 3 \text{ pc}$ (Reines & Deller 2012), also strongly suggests a massive BH. Furthermore, the nuclear source in Henize 2–10 falls along the correlation between nuclear radio and X-ray luminosity for low-luminosity radio galaxies (within the 1σ scatter) found by Panessa et al. (2007).

Our temporal analysis of the nuclear X-ray emission reveals clear variability and a potential ~ 9 hr periodicity. The oscillatory signal is apparent by eye and significant when fitting the light curve. However, the X-ray periodicity is not yet significant when considering the power spectrum, and at present, we cannot distinguish between a true periodic signal and random fluctuations in brightness mimicking a periodic signal during our 160 ks observation (e.g., red noise; see Vaughan & Uttley 2006; Vaughan et al. 2016). Nevertheless, we discuss possible origins for a ~ 9 hr X-ray periodicity below.

The most likely origin is a low-frequency quasi-periodic oscillation (LFQPO; Remillard & McClintock 2006). QPOs are generally thought to arise from instabilities in the accretion flow (e.g., Tagger & Pellat 1999) or geometric oscillations (e.g., Molteni et al. 1996). It has been proposed that LFQPOs may be due to the orbital precession of non-equatorial particles in the dragged spacetime around a spinning BH (i.e., Lense-Thirring precession; Stella & Vietri 1998). Given the timescale of the apparent periodicity and the low luminosity, current observational constraints on such variability are limited, with only a single claimed detection of an LFQPO from a massive BH that is accreting at a relatively high rate ($\sim 0.1 L_{\text{Edd}}$, Lin et al. 2013).

We also considered a high-frequency QPO (HFQPO) as an origin for the X-ray periodicity; however, the observed luminosity and frequency argue against this. The known stellar and massive BH QPO detections that are consistent with an HFQPO origin are all from sources known to be accreting at close to the Eddington limit (e.g., Remillard & McClintock 2006; Gierliński et al. 2008; Reis et al. 2012; Alston et al. 2014, 2015; Pan et al. 2016). HFQPOs are thought to originate in the inner regions of the accretion flow in the immediate vicinity of the BH. The observed relation between QPO frequency and BH mass (e.g., Remillard & McClintock 2006;

⁸ Coincidentally, this is approximately the same mass estimated by Reines et al. (2011) using the BH fundamental plane (Merloni et al. 2003) and the luminosity of the bright variable source that dominated the 2001 *Chandra* observation. Using the luminosity of the nuclear source in our new observation ($L_X \sim 10^{38} \text{ erg s}^{-1}$, when the transient source was “off”) and a 5 GHz radio luminosity of $L_R \sim 4 \times 10^{35} \text{ erg s}^{-1}$ (Reines & Deller 2012), the fundamental plane gives $\log(M_{\text{BH}}/M_\odot) \sim 7 \pm 1$, consistent with the estimate based on the scaling between M_{BH} and M_* from Reines & Volonteri (2015).

Zhou et al. 2015; Pan et al. 2016) would predict a mass of $\sim 10^8 M_\odot$ for a frequency of $f \sim 3 \times 10^{-5}$ Hz, more than an order of magnitude greater than the expected mass of the BH in Henize 2–10.

A final intriguing possibility is orbital variability related to a massive BH binary, where at least one of the BHs is actively accreting, albeit at a low level (Roedig et al. 2012, 2014; Sesana 2013). In this case, the periodicity would correspond to the serendipitous electromagnetic discovery of a massive BH binary with $\lesssim 5$ years until merger, for an assumed total system mass of $\sim 10^6 M_\odot$ (Sesana 2013). Although there is evidence that Henize 2–10 has experienced a merger in the recent past (Kobulnicky et al. 1995), and thus the presence of two massive BHs is possible, we regard this possibility as unlikely given the extremely short timescale until coalescence implied by the observed frequency.

While we consider a weakly accreting massive BH the most likely origin for the nuclear X-ray/radio source in Henize 2–10, we nonetheless revisit alternative explanations including a stellar-mass XRB and/or a young supernova remnant (SNR; also see the Supplementary Information in Reines et al. 2011 as well as the discussion in Reines & Deller 2012). Neither an XRB nor an SNR alone can account for *both* the X-ray and radio properties of the nuclear source. The radio emission is simply too luminous to be produced by an XRB, especially one in the soft thermal state (Fender et al. 2009) as would be indicated by the observed spectrum, and the X-ray variability is incompatible with an SNR. Our constraints on the positions of the nuclear radio and X-ray sources, however, strongly suggest a common/related source. In principle, we can imagine a scenario in which the X-rays originate from an accreting stellar-mass XRB residing within the radio-emitting remnant of the supernova that created the compact object. Given the size and luminosity of the radio source, an SNR would likely be only decades old (Fenech et al. 2010; Reines & Deller 2012) and therefore the nuclear X-ray source would be the new record holder for the youngest XRB known by a wide margin (e.g., Circinus X-1 has an age $t < 4600$ years; Heinz et al. 2013). While we cannot definitively rule out this scenario, we consider it somewhat contrived. Moreover, the radio/X-ray source is at the center of the galaxy (the natural place for a massive BH) and there is no star cluster or recent star formation at the location of the source as would be expected for a young XRB/SNR origin (Reines et al. 2011).

Finally, our study demonstrates the value of X-ray imaging at sub-arcsecond scales and emphasizes the need for a high-resolution next-generation X-ray observatory. Our detection of the first potential LFQPO from a low-luminosity massive BH would not have been possible with any existing X-ray observatory other than *Chandra*. Future studies of this class of objects (e.g., with *ATHENA* and the X-ray Surveyor) would open a new window to study low-luminosity accretion flows, which are the dominant mode of BH accretion on cosmological scales.

We thank Richard Plotkin for useful discussions and the anonymous referee for reviewing our work. A.E.R. is grateful for support from NASA through Hubble Fellowship grant HST-HF2-51347.001-A awarded by the Space Telescope Science Institute, which is operated by the Association of Universities for Research in Astronomy, Inc., for NASA, under contract NAS 5-26555. Support for this work was also

provided by NASA through *Chandra* award number GO4-15098A issued by the *Chandra* X-ray Observatory Center, which is operated by the Smithsonian Astrophysical Observatory for and on behalf of the NASA under contract NAS8-03060. G.R.S. acknowledges support by an NSERC Discovery Grant.

REFERENCES

- Alston, W. N., Markevičiūtė, J., Kara, E., Fabian, A. C., & Middleton, M. 2014, *MNRAS*, **445**, L16
- Alston, W. N., Parker, M. L., Markevičiūtė, J., et al. 2015, *MNRAS*, **449**, 467
- Arca-Sedda, M., Capuzzo-Dolcetta, R., Antonini, F., & Seth, A. 2015, *ApJ*, **806**, 220
- Arnaud, K. A. 1996, in ASP Conf. Ser. 101, *Astronomical Data Analysis Software and Systems V*, ed. G. H. Jacoby & J. Barnes (San Francisco, CA: ASP), 17
- Asplund, M., Grevesse, N., Sauval, A. J., & Scott, P. 2009, *ARA&A*, **47**, 481
- Baganoff, F. K., Maeda, Y., Morris, M., et al. 2003, *ApJ*, **591**, 891
- Baldassare, V. F., Reines, A. E., Gallo, E., & Greene, J. E. 2015, *ApJL*, **809**, L14
- Baldassare, V. F., Reines, A. E., Gallo, E., & Greene, J. E. 2016, *ApJ*, submitted (arXiv:1609.07148)
- Balucinska-Church, M., & McCammon, D. 1992, *ApJ*, **400**, 699
- Constantin, A., Green, P., Aldcroft, T., et al. 2009, *ApJ*, **705**, 1336
- Fender, R. P., Homan, J., & Belloni, T. M. 2009, *MNRAS*, **396**, 1370
- Fenech, D., Beswick, R., Muxlow, T. W. B., Pedlar, A., & Argo, M. K. 2010, *MNRAS*, **408**, 607
- Fruscione, A., McDowell, J. C., Allen, G. E., et al. 2006, *Proc. SPIE*, **6270**, 62701V
- Gehrels, N. 1986, *ApJ*, **303**, 336
- Gierliński, M., Middleton, M., Ward, M., & Done, C. 2008, *Natur*, **455**, 369
- Hainline, K. N., Reines, A. E., Greene, J. E., & Stern, D. 2016, *ApJ*, in press (arXiv:1609.06721)
- Heinz, S., Sell, P., Fender, R. P., et al. 2013, *ApJ*, **779**, 171
- Johnson, K. E., & Kobulnicky, H. A. 2003, *ApJ*, **597**, 923
- Johnson, K. E., Leitherer, C., Vacca, W. D., & Conti, P. S. 2000, *AJ*, **120**, 1273
- Kalberla, P. M. W., Burton, W. B., Hartmann, D., et al. 2005, *A&A*, **440**, 775
- Kobulnicky, H. A., Dickey, J. M., Sargent, A. I., Hogg, D. E., & Conti, P. S. 1995, *AJ*, **110**, 116
- Kobulnicky, H. A., & Johnson, K. E. 1999, *ApJ*, **527**, 154
- Kobulnicky, H. A., & Martin, C. L. 2010, *ApJ*, **718**, 724
- Lemons, S. M., Reines, A. E., Plotkin, R. M., Gallo, E., & Greene, J. E. 2015, *ApJ*, **805**, 12
- Li, J., Kastner, J. H., Prigozhin, G. Y., et al. 2004, *ApJ*, **610**, 1204
- Lin, D., Irwin, J. A., Godet, O., Webb, N. A., & Barret, D. 2013, *ApJL*, **776**, L10
- Merloni, A., Heinz, S., & di Matteo, T. 2003, *MNRAS*, **345**, 1057
- Molteni, D., Sponholz, H., & Chakrabarti, S. K. 1996, *ApJ*, **457**, 805
- Nguyen, D. D., Seth, A. C., Reines, A. E., et al. 2014, *ApJ*, **794**, 34
- Ott, J., Walter, F., & Brinks, E. 2005, *MNRAS*, **358**, 1423
- Pan, H.-W., Yuan, W., Yao, S., et al. 2016, *ApJL*, **819**, L19
- Panessa, F., Barcons, X., Bassani, L., et al. 2007, *A&A*, **467**, 519
- Reines, A., & Comastri, A. 2016, arXiv:1609.03562
- Reines, A. E., & Deller, A. T. 2012, *ApJL*, **750**, L24
- Reines, A. E., Greene, J. E., & Geha, M. 2013, *ApJ*, **775**, 116
- Reines, A. E., Plotkin, R. M., Russell, T. D., et al. 2014, *ApJL*, **787**, L30
- Reines, A. E., Sivakoff, G. R., Johnson, K. E., & Brogan, C. L. 2011, *Natur*, **470**, 66
- Reines, A. E., & Volonteri, M. 2015, *ApJ*, **813**, 82
- Reis, R. C., Miller, J. M., Reynolds, M. T., et al. 2012, *Sci*, **337**, 949
- Remillard, R. A., & McClintock, J. E. 2006, *ARA&A*, **44**, 49
- Roedig, C., Krolik, J. H., & Miller, M. C. 2014, *ApJ*, **785**, 115
- Roedig, C., Sesana, A., Dotti, M., et al. 2012, *A&A*, **545**, A127
- Sesana, A. 2013, *COGRA*, **30**, 244009
- Stella, L., & Vietri, M. 1998, *ApJL*, **492**, L59
- Tagger, M., & Pellat, R. 1999, *A&A*, **349**, 1003
- Vasudevan, R. V., & Fabian, A. C. 2009, *MNRAS*, **392**, 1124
- Vaughan, S., & Uttley, P. 2006, *AdSpR*, **38**, 1405
- Vaughan, S., Uttley, P., Markowitz, A. G., et al. 2016, *MNRAS*, **461**, 3145
- Whalen, T. J., Hickox, R. C., Reines, A. E., et al. 2015, *ApJ*, **806**, 37
- Zhou, X.-L., Yuan, W., Pan, H.-W., & Liu, Z. 2015, *ApJL*, **798**, L5